Design of Performance-Enhanced Fabry-Perot Micro-Cavity Structure With a Novel Single Deeply Corrugated Diaphragm

W. J. Wang, R. M. Lin, D. G. Guo

Centre for Mechanics of Micro-Systems, School of Mechanical & Production Engineering, Nanyang Technological University, Singapore, 639798, mwjwang@ntu.edu.sg

ABSTRACT

A Fabry-Perot micro-cavity structure with a novel single deeply corrugated diaphragm (SDCD) for use as pressure sensors has been demonstrated. Both analytical and finite element methods are used to evaluate the SDCD's improved performance of signal-averaging effect as compared with that of flat diaphragm of identical membrane area and film thickness. The proposed Fabry-Perot pressure sensor has been designed with a single-wafer construction and fabricated using silicon micromachining technologies. The results show reasonable sensor performance in terms of sensitivity and response values.

Keywords: MEMS, Fabry-Perot, pressure sensor, finite element method.

1 INTRODUCTION

Optically interrogated pressure sensors have been demonstrated as an alternative to conventional piezoresistive and capacitive pressure sensors to extend the use of these sensors to harsh environments in which electronics cannot operate. The silicon micromachining technique has been successfully applied to the fabrication of miniature Fabry-Perot sensors [1-3]. This kind of sensor detects changes in optical path length induced by either a change in the refractive index or a change in physical length of the cavity. Micromachining techniques make Fabry-Perot sensors more attractive by reducing the size and the cost of the sensing element. Owing to the small size and the optical interrogation method, a micromachined sensor array that would provide pressure maps with high spatial resolution could be developed. Such sensor arrays could play an important role in medical applications.

In this paper, a novel single deeply corrugated diaphragm (SDCD) structure has been proposed for Fabry-Perot sensor with improved signal-averaging effect compared to the conventional flat diaphragms.

2 SIMULATION OF SDCD STRUCTURE

Figure 1 shows the cross-section of the SDCD structure with geometrical parameters. The SDCD structure consists of a flat membrane that is suspended all around with free-sidewalls (with a 54.74° angle previously formed by anisotropic etching). The flat bottom-region of the bottom diaphragm is believed to behave just like a normal flat diaphragm (FD) with lower stiffness. The suspending sidewalls are expected to behave as a buffer for the moving diaphragm to improve planar movement in the optically sampled area of the cavity. It is also imaginable that the initial stress be partly released with slight variation in shape of the very flexible suspending sidewalls while the SDCD is freed by sacrificial-layer etching.

There is no reported analytical expression of deflection due to the application of pressure for this type of diaphragm in the open literature. For the purpose of considering the effect of the improved mechanical compliance by decreasing mechanical stiffness of the diaphragm and releasing the initial stress, correction factors C_{f1} and C_{f2} are introduced in the deflection of a conventional FD due to the application of pressure P, and the analytical expression of the deflection of a SDCD structure is expressed as

$$W_m = \frac{a^2 P}{\pi h\left[C_{f1}\,\pi E h^2/3a^2\left(1-\upsilon^2\right)+C_{f2}\sigma\pi\right]} \quad (1)$$

where a is the half side length of the square diaphragm, h diaphragm thickness, υ is Poisson ratio of silicon, E is Young's modulus of silicon and σ the initial stress of the diaphragm, respectively. Both C_{f1} and C_{f2} are expected to be smaller than one and, will decrease with the increase in corrugation depth.

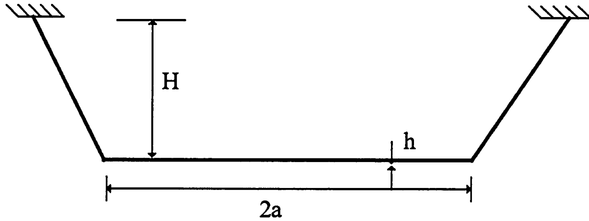

Figure 1: Schematic cross-section of the SDCD structure with geometrical parameters.

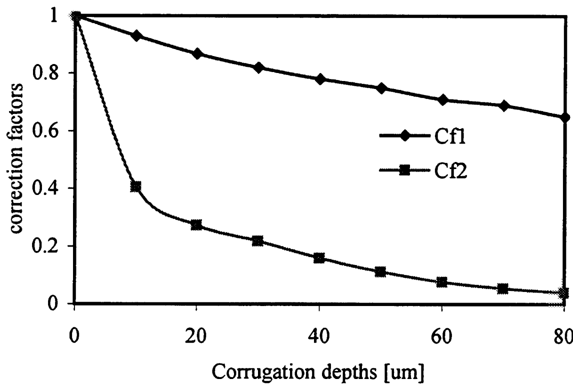

Figure 2: Evaluation of corrective factors of C_{f1} and C_{f2} vs. the depth of the single corrugation, from FEM simulation results.

FEM simulation has been used to confirm the effects of the SDCD structure. The initial stress of the diaphragm is induced by the equivalent cooling temperature method as proposed by Zhang and Wise [4]. Both the conventional FD of 100 μm x 100 μm area and 1.6 μm thickness, as well as, the SDCDs of identical bottom area and thickness but various corrugation depths are simulated using ANSYS 5.6.

Figure 2 shows the extracted correction factors C_{f1} and C_{f2}, which are obtained from the FEM results under the stress-free condition and an initial stress of 90 Mpa. The results clearly confirm that either of the two factors is <1 and decreases with increase in corrugation depth.

3 DESIGN

The proposed Fabry-Perot pressure sensor is schematically shown in Figure 3. It consists of four major components: a top diaphragm that also serves as one of the mirrors of the Fabry-Perot cavity; an air gap between the mirrors of the cavity; a bottom diaphragm that forms the other mirror; and a mechanical structure that holds and aligns the optical fiber to the micromachined cavity.

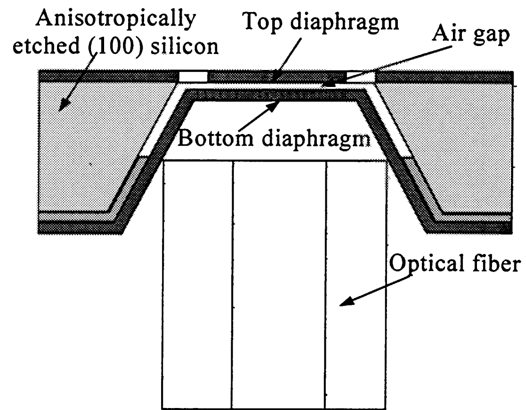

Figure 3: Cross-sectional view of the Fabry-Perot sensor with two flexible mirrors.

The Fabry-Perot cavity is monolithically built by etching a sacrificial layer that lies between the top and bottom dielectric diaphragms. The gap of the cavity can be precisely adjusted by controlling the thickness of a sacrificial layer grown using LPCVD. The technique allows for batch fabrication of the pressure sensors with excellent alignment and parallelism of the two mirrors in the cavity. This alignment has been a problem in previous devices that use a hybrid assembly technique.

To design a micromachined Fabry-Perot cavity pressure sensor, the key design parameters of mechanical travel of the moving mirror and the initial gap of the Fabry-Perot cavity should be carefully selected.

The mechanical travel can be determined according to the desired pressure range and the mechanical compliance of the moving mirror. This in turn can be determined by the

thickness and lateral dimension of the bottom diaphragm that forms the moving mirror in the sensor.

The diaphragm consists of a multiple film stack of two silicon nitride layers cladding a silicon dioxide layer. The thickness of each layer in the dielectric stack affects both the residual stress in the diaphragms and the optical response of the cavity. The thickness of each layer is chosen in such a way that the Fabry-Perot microcavity is mechanically stable, i.e., it should not buckle or crack, and must have optimal characteristics of the optical response. The thickness ratio of silicon dioxide to silicon nitride is optimized to be about 4 to 6, experimentally. With the ratio of 4 to 6, the equivalent residual stress of the composite stack is slightly under tension.

The size of the flat region of the SDCD structure is chosen to be smaller than the diameter of the optical fiber so that during fiber insertion the (111) planes of the etched groove serve as mechanical stops preventing the fiber from actually contact the flat region of the SDCD. Since the lateral dimensions are set by the fiber alignment structure, compliance would be adjusted mainly via changes in the diaphragm thickness.

As an example, calculations indicated that at a wavelength of $\lambda = 850$ nm, the diaphragm thickness required for making a diaphragm deflection of $\lambda/4$ at 10 psi was 1.60 μm. This calculation was done for the diaphragm with corrugation depth of 80 μm and side length of 100 μm.

For Fabry-Perot sensors, the gap g should be carefully selected to obtain linear response over the desired pressure range. Using the characteristic matrix method, the reflectance R of the structure can be found from[5]:

$$R = \left| \frac{\eta_{in} B - C}{\eta_{in} B - C} \right|^2 \qquad (2)$$

where

$$\begin{bmatrix} B \\ C \end{bmatrix} = \left(\prod_{i=1}^{q} \begin{bmatrix} \cos(k_o n_i z_i) & \frac{j}{\eta_i} \sin(k_o n_i z_i) \\ j\eta_i \sin(k_o n_i z_i) & \cos(k_o n_i z_i) \end{bmatrix} \right) \begin{bmatrix} 1 \\ \eta_f \end{bmatrix} \qquad (3)$$

with $k_0 = 2\pi / \lambda_0$. η_f and η_{in} are the admittances of the environment outside the sensor and of the medium from which the light comes, respectively. n_i and z_i are the refractive index and thickness of the ith layer, respectively.

Determination of this variable usually requires additional constraints imposed by the manufacturing process. For example, initial gap should be carefully selected to maximize yield when layer thickness variation due to the manufacturing process is considered. With a proper combination of initial cavity length and mechanical travel the optical response of the cavity becomes the least sensitive to process-induced thickness variations in the layers of the cavity.

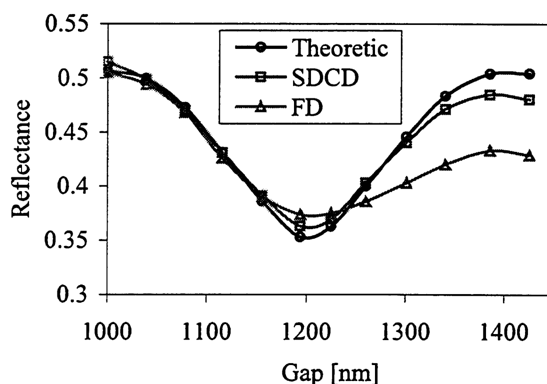

Figure 4: The simulated reflectance versus the gap at the center of the diaphragm.

Figure 4 shows the simulated reflectance versus the gap at the center of the diaphragm. The reflectance of the first peak at 1000 nm is about 18% higher than that of the second peak at about 1420 nm for the flat diaphragm. This is due to the signal-averaging effect. However, the reflectance of the first peak at 1000 nm is about 5% higher than that of the second peak at about 1420 nm for the SDCD structure, which demonstrates the parasitic signal-averaging effect can be reduced by using SDCD structure. This reduction is achieved by enhancing the flatness of the deflecting diaphragm within the optically sampled area.

4 FABRICATION AND MEASUREMENTS

The Fabry-Perot pressure sensor is fabricated using both surface and bulk micromachining techniques. The top

diaphragm dielectric stack of the Fabry-Perot cavity consisting of Si_xN_y(0.15 μm)-SiO_2 (0.9 μm)-Si_xN_y (0.15 μm) is deposited directly on top of the n-type double-sided polished (100) wafer. The dielectric stack deposited on the backside of the wafer is patterned and the deep groove is etched with 40% aqueous KOH at 60 °C. Then, about 1 μm thick LPCVD undoped polysilicon layer is deposited. This layer will serve as the sacrificial-layer for diaphragm release. The SDCD dielectric stack consisting of Si_xN_y (0.2 μm)-SiO_2(1.2 μm)-Si_xN_y (0.2 μm) is LPCVD formed over the sacrificial layer. During both the polysilicon and the dielectric diaphragm deposition steps, the front side is protected to prevent deposition on the top diaphragm. The resultant tensile residual stresses of the stacked layers of the diaphragms are measured as 90Mpa. The stress of the film at every process stage is obtained by measuring a dummy wafer using a curvature-based film-stress meter. The SEM micrograph in Figure 5 shows the cross-section of a released suspension-sidewall.

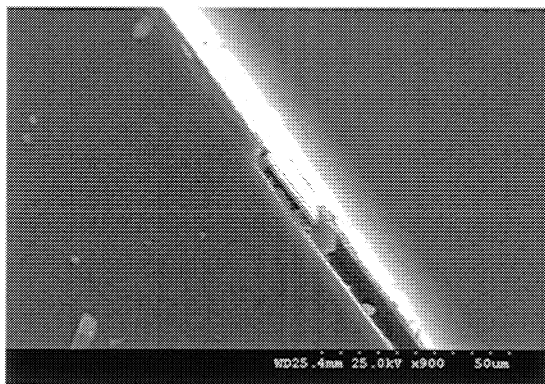

Figure 5: SEM micrographs showing the cross-section of a released suspension-sidewall.

An applied pressure deflects the diaphragms and changes the optical path length of the cavity, which is sensed by the change in the intensity of the light transmitted through or reflected from the sensor. The sensor response results are shown in Figure 6. The results show reasonable sensor performance in terms of sensitivity and response values. The validity of the calculated deflection distance of the bottom mirror is evaluated by comparing with the extracted deflection distance from the transmittance plot. The calculated deflection distance of the SDCD mirror, 433 nm, is comparable with the one peak-to-peak period of the transmittance, 425 nm.

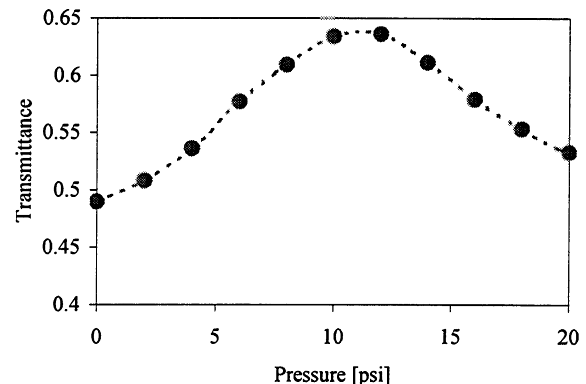

Figure 6: Plot of sensor output in volts versus pressure in psi for the Fabry-Perot sensor.

REFERENCES

[1] Y. Kim, D. P. Neikirk, Micromachined Fabry-Perot cavity pressure transducer, IEEE Photonics Technology Letters, 7 (12), 1995.

[2] D. C. Abeysinghe, S. Dasgupta, J. T. Boyd, and H. E. Jackson, A novel MEMS pressure sensor fabricated on an optical fiber, IEEE Photonics Technology Letters, **13** (9), 2001.

[3] J. Han and D. P. Neikirk, Deflection behavior of Fabry-Perot pressure sensors having planar and corrugated membrane, SPIE's Micromachining and Microfabrication '96 Symposium: Micromachined Devices and Components II, R. Roop and K. Chau, Proc. SPIE 2882, Austin, Texas, USA, 14-15 October, 1996, pp. 79-90.

[4] Y. F. Zhang and K. D. Wise, Performance of Non-Planar Silicon Diaphragms under Large Deflections, *J. of Microelectromechanical systems*, **3**, 59-68, 1994.

[5] M. Born, E. Wolf, Principles of optics, Pergamon Press, Oxford, 1980.